Journal of Applied Geophysics 66 (2008) 15–24

Contents lists available at ScienceDirect

Journal of Applied Geophysics

journal homepage: www.elsevier.com/locate/jappgeo

V_S and V_P vertical profiling via joint inversion of Rayleigh waves and refraction travel times by means of bi-objective evolutionary algorithm

Giancarlo Dal Moro *

Department of Geological, Environmental and Marine Sciences Exploration Geophysics Group University of Trieste via Weiss, 1, 34127 Trieste – Italy

ARTICLE INFO

Article history:
Received 27 April 2007
Accepted 5 August 2008

Keywords:
Joint inversion of seismic data
Multi-objective problems
Evolutionary algorithms
Pareto front
Surface wave dispersion
Refraction seismics, Genetic algorithms
Poisson ratio

ABSTRACT

Rayleigh wave dispersion curves and refraction travel times are jointly inverted through a procedure based on a Multi-Objective Evolutionary Algorithm (MOEA) technique. The proposed procedure aims at improving the reconstruction of subsurface structure by exploiting the complementary information attainable by refraction seismics and surface-wave dispersion and by overcoming in this way the problems related to non-uniqueness of the solution (surface waves and refraction seismics) and hidden layers (refraction).

The proposed scheme allows the joint inversion of the data and the validation of the provisional interpretation. In fact, Pareto front symmetry proves to be a valuable tool to verify the coherency of the adopted interpretation as an incorrect number of layers, refractor attribution or assumed Poisson values reflect in non-symmetric Pareto front as well as in wider model distribution in the objective space.

Methodology is initially tested using synthetic data and successfully applied to a field dataset resulting from a single standard seismic survey with vertical geophones and vertically-incident seismic source (sledgehammer).

1. Introduction

Surface wave dispersion has been used for crustal studies since the 50s (e.g. Evison et al., 1959) and, more recently, for near-surface seismic characterization (Stokoe et al., 1988; Glangeaud et al., 1999; Park et al., 1999; Xia et al., 1999; Louie, 2001; Dal Moro et al., 2007).

Among the several appealing characteristics of the methods based on Surface Wave (SW) analysis we can recall:

- the high amplitude that make them suitable for noisy (e.g. urban) areas;
- the minor attenuation with respect to body waves;
- the easy generation: a large fraction of the energy produced by standard vertically-incident seismic sources actually propagates as SW;
- the little interpretative effort (with respect to reflection and refraction surveys);
- the absence of the blind-zone problem, unlike refraction seismics;
- the final result is the vertical shear-wave profile (crucial for several engineering applications)

On the other hand, the main problem is related to the highly multi-modal (i.e. non-uniqueness) nature of the dispersion curve inversion that mirrors in the need for a careful evaluation of the final results (e.g. Luke et al., 2003).

Fig. 1 shows the vertical V_S profiles and dispersion curves of six models. Dispersion curves are plotted over the velocity spectrum of a field dataset obtained from a site characterized by an 18 m unconsolidated sequence laying over a hard bedrock. At a depth of 15 m velocities range from about 290 to 550 m/s while at 30 m from 400 up to 2000 m/s (Fig. 1a). Related dispersion curves (Fig. 1b) are nevertheless extremely similar in the 5–17 Hz range and give a clear evidence of the so-called non-uniqueness of the solution.

In addition, velocity spectrum evaluation must be performed by carefully considering possible artefacts or misleading features such for instance misinterpreted modes (Zhang and Chan, 2003) or guided waves, reflections etc. (Robertsson et al., 1995; Roth and Holliger, 1999; Dal Moro et al., 2006).

On the other hand, also refraction studies suffer from two problems: the hidden layer (also referred to as "blind zone") (e.g. Soske, 1959) and the non-uniqueness of the solution (Ivanov et al., 2005a,b).

Furthermore as small variations of the picked travel times can result, especially for refractions from high-velocity layers, in large differences in the retrieved models, data interpretation is an error-prone task subject to personal (mis)interpretations of the interpreter.

In order to tackle these problems in an integrated perspective Ivanov et al. (2006) proposed to use a model retrieved from Rayleigh-wave analysis as reference model to invert refraction travel times.

Multi-Objective Evolutionary Algorithms (MOEAs) offer a tool for a joint inversion of multi-datasets and, to some extent, provide a series

* Corresponding author. Tel.: +39 040 5582287; fax: +39 040 5582290.
E-mail address: dalmoro@units.it.

0926-9851/$ – see front matter © 2008 Elsevier B.V. All rights reserved.
doi:10.1016/j.jappgeo.2008.08.002

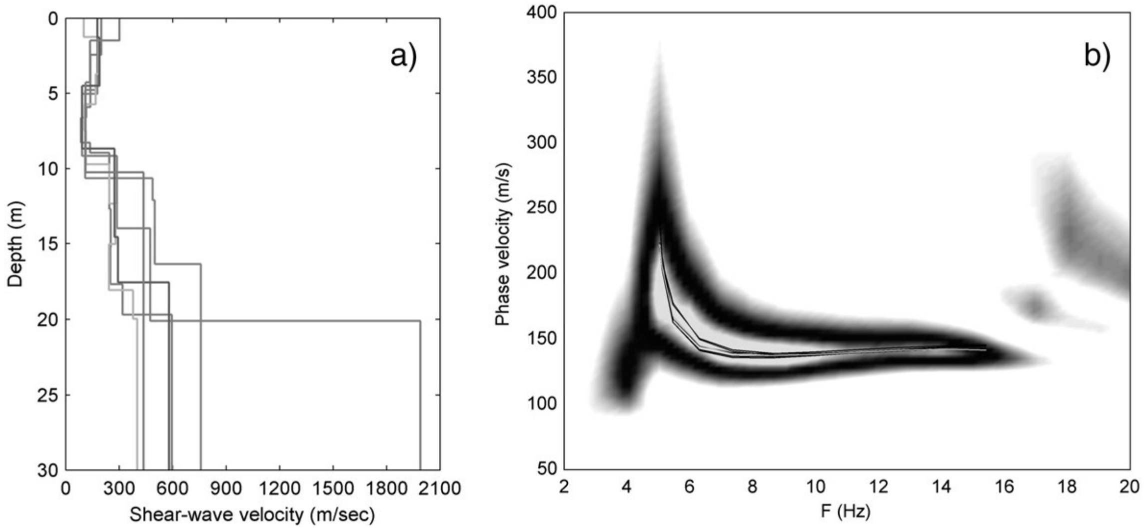

Fig. 1. (a) A series of vertical shear-wave profiles and (b) their dispersion curves in the 5–17 Hz frequency range. In the background an observed velocity spectrum for a site characterized by an 18 m unconsolidated-sediment sequence laying over a hard bedrock.

of ancillary information able to give the user the opportunity to assess whether the provisional interpretation is appropriate or not.

In fact, if the preliminary data interpretation is not correct (e.g. erroneous interpretation of reflectors/refractions with respect to the chosen subsurface model) incongruities arise from the optimization procedure and give the user the chance to realize the problem (Dal Moro and Pipan, 2007).

In other words, the proposed scheme allows the evaluation of the consistency of the inversion itself (i.e. the inherent provisional data interpretation).

As a matter of fact, the present study represents a follow-up of a previously-published work (Dal Moro and Pipan, 2007) in which the authors explored the potential of bi-objective evolutionary algorithms for the joint inversion of SH-wave reflection travel times and Rayleigh wave dispersion curves.

In the present paper the methodology proposed in Dal Moro and Pipan (2007) for Rayleigh waves and SH-wave reflection travel times is applied to jointly invert dispersion curves and refraction travel times.

The idea of jointly inverting surface waves and refraction travel times was suggested by the fact that good reflections are not a common feature in vertical-component geophone surveys – Dal Moro and Pipan (2007) considered SH-wave datasets – while refractions are definitely more-easily detected. On the other side refraction surveys pose serious interpretative problems related to first-break interpretations, hidden layers (low-velocity channels) and non-uniqueness and could highly benefit from the integration of auxiliary data such as surface waves.

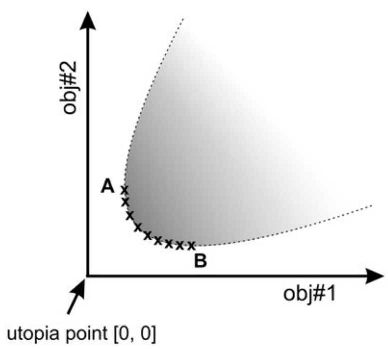

Fig. 2. Objective space for a typical bi-objective problem. Crosses represent the Pareto front models.

Consequently, the perspective of the present study is the one we normally assume when performing a standard P-wave survey (vertical-component geophones) in which refraction event(s) and *ground roll* are usually very clear.

The, so to speak, handicap that must be faced is represented by the fact that *ground roll* is mainly related to shear-wave velocity (Xia et al., 1999) while refracted waves just to acoustic-wave velocity. Thickness of the layers is a decisive parameter for both the events.

As a consequence, a proper strategy is required to reasonably handle and invert the dataset. If the inversion procedure is properly designed, it is possible to estimate Poisson moduli and overcome the mentioned problems of non-uniqueness and blind zone.

For the sake of brevity, in the present paper we will not review the entire theoretical background of MOEA. Only the major facts will be briefly recalled while in order to gain a deeper insight into the methodology and the paradigms to adopt to evaluate the results the reader can refer to Dal Moro and Pipan (2007).

2. Methodology

Soft computing techniques represent a way to approach data analysis and optimization by means of fuzzy and approximate methods that are particularly suitable for highly-complex problems whose solution cannot be sought via common analytical approaches (Wong et al., 2002).

Most of such methods (e.g. tabu search, evolutionary algorithms, ant colony search, simulated annealing etc.) are largely based on random processes driven towards an optimal solution. The way the optimization is obtained characterizes each specific method. In genetic (or evolutionary) algorithms (GAs or EAs) such optimization

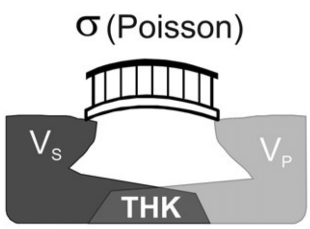

Fig. 3. Informal graphical representation of the structure of the present MOP.

Table 1
Parameters of the synthetic model adopted for the tests: V_S and V_P the shear- and compressional-wave velocities, ρ the density and THK the thickness

		V_P (m/s)	V_S (m/s)	THK (m)	Poisson	ρ (g/cm^3)
Layer	1	700	285	3	0.4	1.97
	2	400	163	2	0.4	1.83
	3	1470	600	10	0.4	2.15
	4	2300	1328	*half-space*	0.25	2.26

is performed along several steps (defined *generations*) through the application of three operations: *selection*, *crossover* and *mutation* (e.g. Goldberg, 1989; Man et al., 2001).

Among the several relevant aspects characterizing GAs we must mention the fact that they are much less prone to local-minimum failure than the traditional gradient-based methods.

In other words, if the function we are considering has several local minima, gradient-based methods will furnish a final solution depending on the adopted starting model that will be necessarily attracted towards the nearest minimum.

On the other side, heuristic methods do not require any starting model and explore a user-defined search space seeking for the global minimum. In case of very complex problems involving several variables and minima, the computational load becomes massive and optimal solution cannot be guaranteed. In such conditions particular strategies should be adopted and final solutions evaluated via statistical tools (Gerstoft and Mecklenbrauker, 1998; Dal Moro et al., 2007).

To properly handle the non-commensurable nature of the two objectives considered for the present study (surface waves dispersion curves and refraction travel times) the same approach adopted in Dal Moro and Pipan (2007) was considered. A bi-objective system based on the Pareto front determination was set up in the framework of a GA scheme (Fonseca and Fleming, 1993, Van Veldhuizen and Lamont, 1998a,b, 2000; Coello Coello 2002, 2003; Dal Moro and Pipan, 2007). A vector $\vec{\boldsymbol{u}} = (\boldsymbol{u}_1, \boldsymbol{u}_2, \ldots, \boldsymbol{u}_k)$ is said to dominate $\vec{\boldsymbol{v}} = (\boldsymbol{v}_1, \boldsymbol{v}_2, \ldots, \boldsymbol{v}_k)$ if and only if $\vec{\boldsymbol{u}}$ is partially less than $\vec{\boldsymbol{v}}$, that is:

$$\forall i \in \{1, \ldots, k\}, u_i \le {}_{vi} \wedge \exists i \in \{1, \ldots, k\} : u_i < v_i \tag{1}$$

where k represents the number of considered objective functions.

A solution $x \in \Omega$ (the decision variable space) is said to be *Pareto optimal* with respect to the universe Ω if and only if there is no $x' \in \Omega$ for which $\vec{\boldsymbol{v}} = F(x')$ dominates $\vec{\boldsymbol{u}} = F(x')$.

For a given MOP (Multi Objective Problem) the ensemble of undominated solutions defines the *optimal Pareto set P* while the *Pareto Front PF* is then defined as

$$\mathrm{PF} := \{\vec{\boldsymbol{u}} = F(x) = (f_1(x), \ldots, f_k(x)) | x \in P\} \tag{2}$$

For non-highly conflicting objectives the typical distribution of models in the objective space is reported in Fig. 2.

The distribution of the models depends on the relationships between the two objectives and can be used to evaluate the provisional data interpretation adopted to invert the data (Dal Moro and Pipan, 2007). In the present case the interpretative aspects are the adopted number of strata. assumed Poisson values and the identification of the refractor a given set of travel times is attributed to.

As we will show in the following paragraphs, in case of errors in the provisional interpretation the model distribution in the objective space is actually deformed from the “normal” distribution represented in Fig. 2. Such anomalous distributions is adopted as a warning indicator of erroneous data interpretation (see Dal Moro and Pipan, 2007).

We considered the Pareto dominance criterion in the framework of an optimization scheme based on an evolutionary algorithm: a ranking process can be adopted in order to identify the fittest models and proceed with the optimization procedure through the application of the genetic operations of *selection crossover* and *mutation*.

In the proposed procedure the rank of a given model is defined on the basis of the number of models that are dominated by it. Genetic procedures are then performed on the individuals (i.e. the models) characterized by the best ranks. Such operations are performed for a number of times (the *generations*) specified by the user (for details see Dal Moro and Pipan, 2007).

3. Objective functions and strategy

The two considered objective functions were defined similarly to the ones adopted in Dal Moro and Pipan (2007). The *root-mean-square* (*rms*) misfit between the observed and calculated dispersion curves

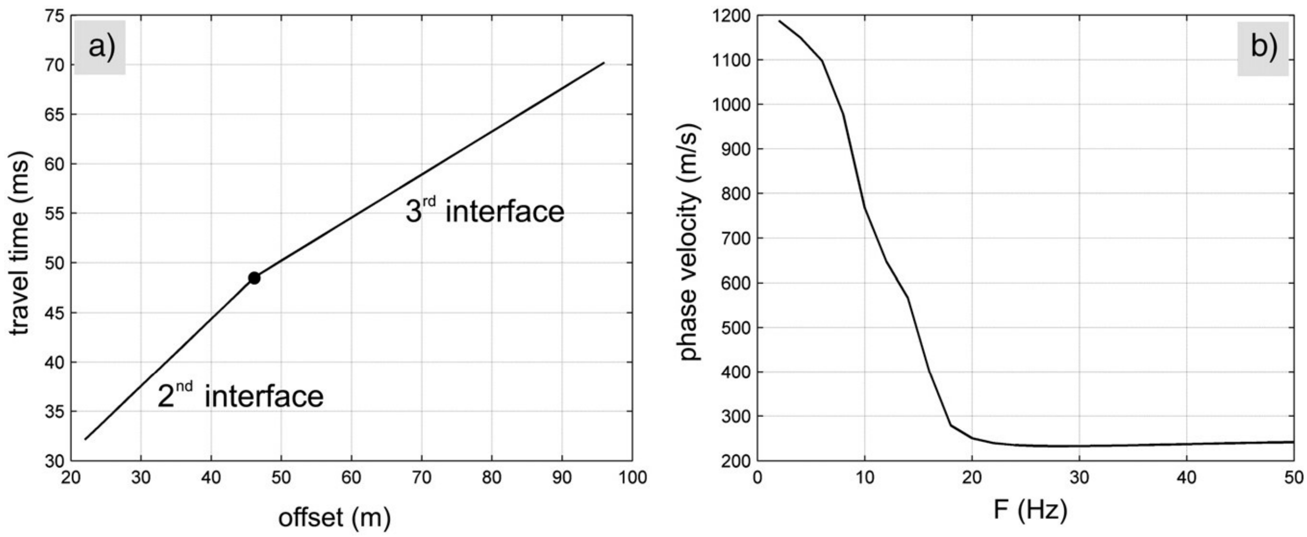

Fig. 4. Synthetic model (see Table 1): (a) travel times of the indicated horizons (due to the velocity inversion the first interface does not generate any refraction event) and (b) dispersion curve.

Table 2
Genetic parameters adopted for the performed inversions

Population size	100
Crossover rate	0.7
Mutation rate	0.1
Number of generations	300
Crossover type	Intermediate recombination
Selection type	Roulette wheel selection
Selection pressure	1.2

Table 4
Search space for case#2 (correct travel time interpretation). Density was fixed according to Eq. (6)

		V_S (m/s)	Poisson (±10%)	THK (m)
Layer	1	200÷400	0.4	1÷5
	2	80÷300	0.4	1÷5
	3	300÷900	0.4	5÷15
	4	900÷1800	0.25	*half-space*

(first objective, hereafter obj#1) and refraction travel times (second objective, hereafter obj#2) are defined according to the following expression:

$$\mathrm{obj} = \sqrt{\frac{\sum_{i=1}^{n}\left(\phi_{\mathrm{obs}_i} - /_{\mathrm{cal}_i}\right)^2}{n}} \tag{3}$$

where Φ represents the Rayleigh-wave phase velocities (obj#1) or the refraction travel times (obj#2) and n is the number of points for the given objective.

As far as obj#1 (dispersion curve misfit) is concerned, the ith misfit (referring to the f_i frequency) is multiplied by a factor w_i calculated as:

$$w_i = \sqrt{\frac{f_i}{f_\mathrm{M}}} \tag{4}$$

where f_M represents the maximum frequency of the considered dispersion curve.

Such a weighting factor is introduced in order to avoid that the higher misfits occurring at the lower frequencies would dominate over the smaller misfits of the higher frequencies (thus possibly determining a loss of resolution for the shallowest layers)

As previously mentioned, the nature of the considered objectives represents a critical and challenging factor for the solution of the system. It is well-known that Rayleigh wave dispersion (obj#1) is mainly a function of shear-wave velocity V_S and thickness THK, while density ρ and V_P play a minor role (Xia et al., 1999).

On the other side, obj#2 depends purely on V_P and THK. This determines a problem whose solution is definitely trickier than the case faced by Dal Moro and Pipan (2007) for the joint inversion of Rayleigh waves and S-wave reflection travel times. In the previous case V_P plays a definitely-minor role while in the present one the V_P/V_S ratio represents a critical aspect, since the two objectives depend on different-but-related velocities. Thickness THK is a common variable while the link between V_S and V_P is clearly represented by the Poisson values (Fig. 3).

The optimization algorithm must then be able to properly perform the search through a reasonable and congruent strategy.

After a number of tests, it was decided to link V_P and V_S by means of a user-defined sequence of Poisson ratios σ (a value for each layer) fixed together with an uncertainty value (μ). In this way, a range of Poisson values $[\sigma-\mu(\sigma)\ \ \sigma+\mu(\sigma)]$ is allowed for each layer. Such relationships are considered both in the generation of the initial random models both in the *crossover* and *mutation* operations that occur in the successive generations.

The individuals (i.e. the models) originated by these two operations are checked to detect anomalous Poisson ratios. If σ exceeds the imposed limits, we consider V_S the leading parameter and adjust V_P on the basis of a Poisson value randomly generated within the imposed limits:

$$V_P = V_S\left(\frac{\sqrt{1-\sigma}}{\sqrt{1/2-\sigma}}\right) \tag{5}$$

It is noteworthy to remember that because of the nature of the involved equations a 5% change in the Poisson value produces a correspondent V_P change of about 10%.

The classical Gardner's et al. (1974) empirical V_P–ρ relationship is adopted to fix the density values:

$$\rho = \log\left(0.23 + (kV_P)^{0.25}\right) \tag{6}$$

where k=1/0.3048 is a constant to convert feet into meters.

It must be underlined that dispersion curves do not give any information about the number of layers while refraction travel times in principle could, even though Ivanov et al. (2005a,b) put in evidence non-uniqueness problems in refraction seismics as well.

Direct wave and V_R at the higher frequencies (of the dispersion curve) can be used to determine P- and S-wave velocities of the uppermost layer.

Similarly to the approach followed in Dal Moro et al. (2007) and Dal Moro and Pipan (2007), we defined a mean model based on the *Marginal Posterior Probability Density* (MPPD).

Actually, MOPs characteristically do not have a single solution but rather a set of solutions (the *optimal Pareto set*) that, for practical uses, can be averaged in order to obtain a single mean model.

4. Joint inversions

The results of some tests performed on a synthetic dataset (Table 1 and Fig. 4) are initially presented and furnish some conceptual schemes useful to discuss the results obtained for a real case successively reported.

We performed data inversions by considering the genetic parameters reported in Table 2 and the constrains and search space summarized in Tables 3 and 4 for the synthetic case and Table 6 for the field dataset.

4.1. Synthetic dataset

In order to test the methodology and evaluate its performances we considered the 4-layer synthetic model reported in Table 1 and Fig. 4.

The adopted model was designed in order to reproduce a typical hidden-layer case which is clearly prone to erroneous refraction travel time interpretation.

Clearly, as the first interface does not produce any refraction due to the velocity inversion, refraction travel times actually due to the

Table 3
Search space for case #1 (erroneous interpretation). Density was fixed according to equation (6). Search space limits for V_P are determined according to the fixed Poisson values (and their uncertainty)

		V_S (m/s)	Poisson (±10%)	THK (m)
Layer	1	200÷450	0.4	4÷10
	2	450÷1000	0.4	6÷14
	3	1000÷2000	0.25	*half-space*

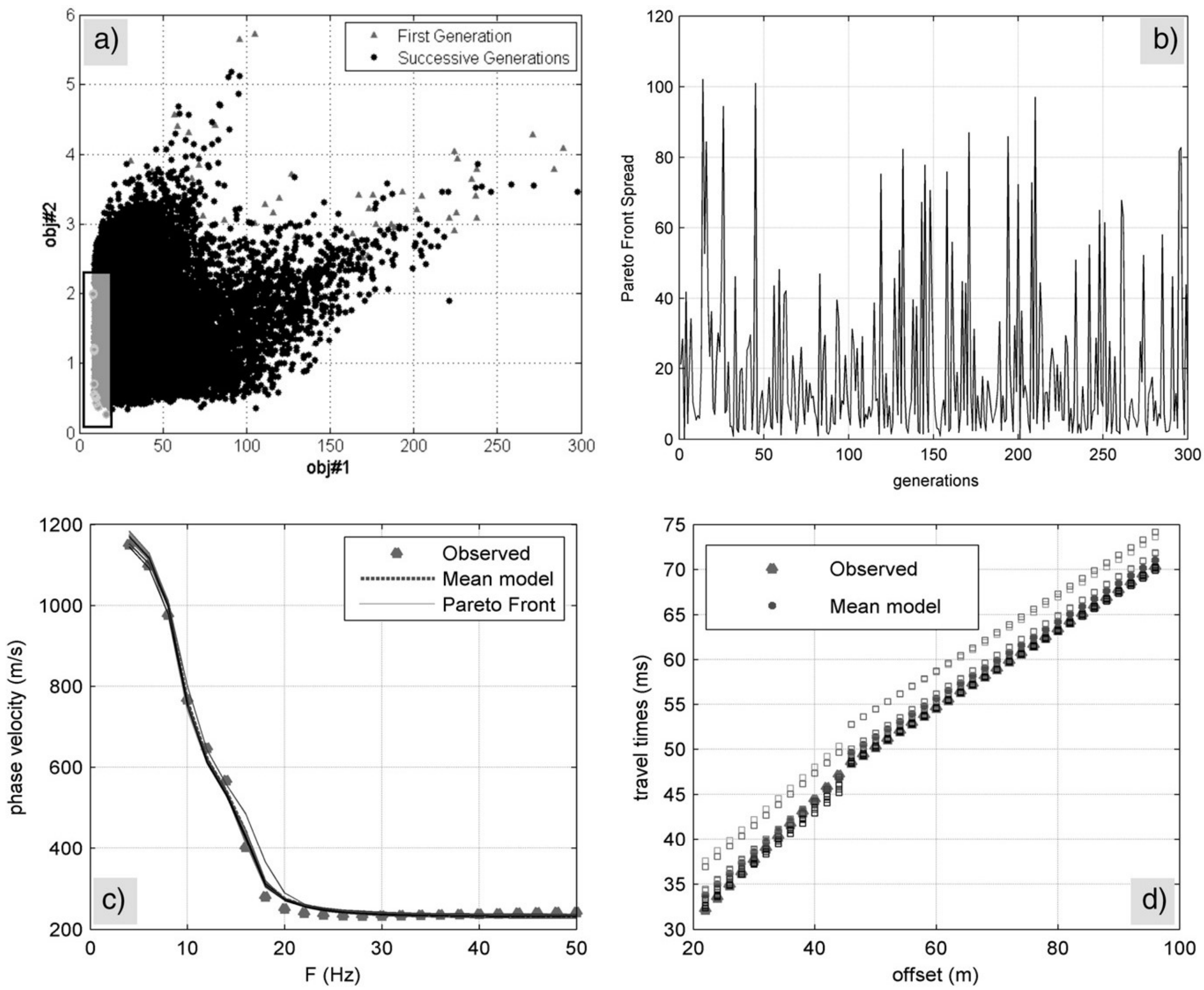

Fig. 5. Synthetic dataset (case #1): bi-objective inversion when a 3-layer model is adopted (see Table 3): a) model distribution in the objective space (Pareto front models highlighted by circles within the rectangle), b) Pareto front length, c) and d) observed and calculated data (dispersion curve and refraction travel time).

second and third interfaces risk to be misinterpreted thus leading to erroneous vertical-profile reconstruction (Fig. 4a).

In order to investigate this scenario we performed two inversions while assuming two different data interpretations. For the first inversion we intentionally assumed an erroneous 3-layer structure (case #1) for which the first and second interfaces were responsible for refraction travel times actually belonging to the second and third horizons.

The second inversion (case #2) is based on a correct assumption (4-layer model) and assumes the possible presence of a hidden layer.

4.1.1. Case #1: Erroneous travel time interpretation

An erroneous structure (2 layers on a *half space*) can be easily derived from the two observed refractions (Fig. 4a). The observed travel times would lead to a structure characterized by $V_{P2}=1470$, $V_{P3}=2300$ m/s (actually pertinent to the third and forth layers) and layer thickness of about 7 and 10 m.

Reasonable Poisson values could then be used to define plausible shear-wave velocities necessary to define a search space to adopt for the inversion (used to optimize the final solution). Direct wave can be used to constrain the first-layer velocity. The resulting search space is summarized in Table 3.

Main outputs of the performed inversion are reported in Fig. 5. Pareto front length is calculated as the sum of the distances between adjacent Pareto front models (see also Dal Moro and Pipan, 2007).

The asymmetry of the Pareto front gives clear indication of the interpretative error, as explained in detail by Dal Moro and Pipan (2007). The nature of the objective functions clearly indicates that the error is connected to the wrong assumption in refractor identification. Due to the severe non-uniqueness of the dispersion curve inversion obj #1 is actually quite fault tolerant while obj #2 will spread along a wider range of values in case of errors, being unable to converge towards a stable solution.

As a consequence, the asymmetry observed for all the tests performed by erroneously varying number of layers, refractor attribution and/or assumed Poisson values is similar to the one reported in Fig. 5a.

4.1.2. Case #2: Correct travel times interpretation

A further inversion was performed according to a proper data interpretation and a 4-layer structure, based on the hypothesis of a hidden layer (see parameters reported in Table 2). Refraction travel times were properly attributed to the second and third horizon and the inversion was performed according to the search space reported in Table 4. Results are shown in Fig. 6 and final mean models reported in Table 5.

The evolution of the Pareto front is different from the trend observed for the joint inversion of Rayleigh wave dispersion curves and SH-wave reflection travel times (Dal Moro and Pipan, 2007). In the

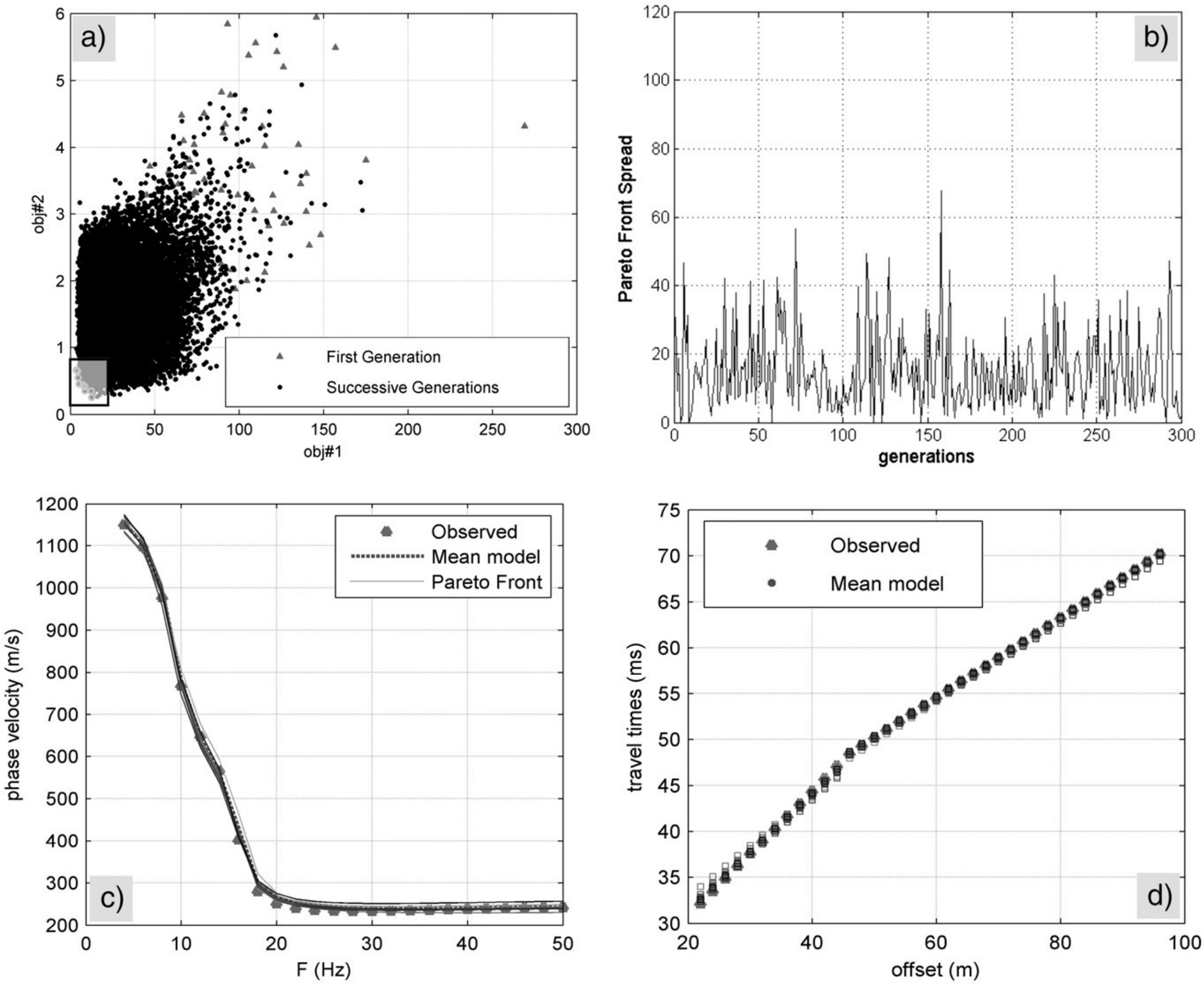

Fig. 6. Synthetic dataset (case #2): bi-objective inversion in case of proper data interpretation (see Table 4): a) model distribution in the objective space (Pareto front models highlighted by circles within the rectangle), b) Pareto front length, c) and d) observed and calculated data (dispersion curve and refraction travel time).

present case, even though the absolute values are smaller when the proper data interpretation is considered (compare Figs. 5b and 6b), the evolution of the Pareto front length (and the objective functions) over the generations do not show any clear decreasing trend that could serve as indicator of a proper preliminary data interpretation — see Figs. 5b and 6b and compare with the results presented in Dal Moro and Pipan (2007).

Nevertheless, model distribution in the bi-objective space and Pareto front symmetry give clear evidence that the solution is correct (see also Dal Moro and Pipan, 2007). The symmetric distribution of the Pareto front models and the smaller scattering of the entire model population can therefore be considered as a robust criterion to evaluate the reliability of the obtained solution and the coherency of the provisional data interpretation (compare Figs. 5a and 6a).

Table 5
Mean models obtained from the erroneous (case #1) and correct (case #2) interpretations (see for comparison the synthetic model summarized in Table 1)

Case	V_P (m/s)	V_S (m/s)	THK (m)	Poisson
#1 (erroneous)	626	247	7.0	0.408
	1791	882	10.3	0.340
	2340	1345	*half-space*	0.253
#2 (correct)	661	270	3.0	0.399
	527	214	3.0	0.401
	1611	661	9.6	0.399
	2304	1332	*half-space*	0.249

4.2. Field dataset

The proposed procedure was then used to invert a field dataset from a sandy beach in NE-Italy. Fig. 7 reports the main acquisition parameters, the considered P-wave common-shot gather with a close-up on the first arrivals and the calculated velocity spectrum.

A preliminary evaluation of the data would give evidence of two refractors and a simple 3-layer model (2 layers on *half-space*) would be then potentially adequate to explain the observed data.

In Fig. 8 the observed velocity spectrum is reported together with the theoretical dispersion curve for a 3-layer model characterized by V_S equal to 87, 335 and 1014 m/s and thicknesses of 3.5 and 4 m (last layer is a *half-space*).

Such data, together with the P-wave velocities obtained from the two observed refraction events (V_P approximately equal to 1400 and 2500 m/s), correspond to Poisson values of 0.47 and 0.40 for the second and third layers respectively.

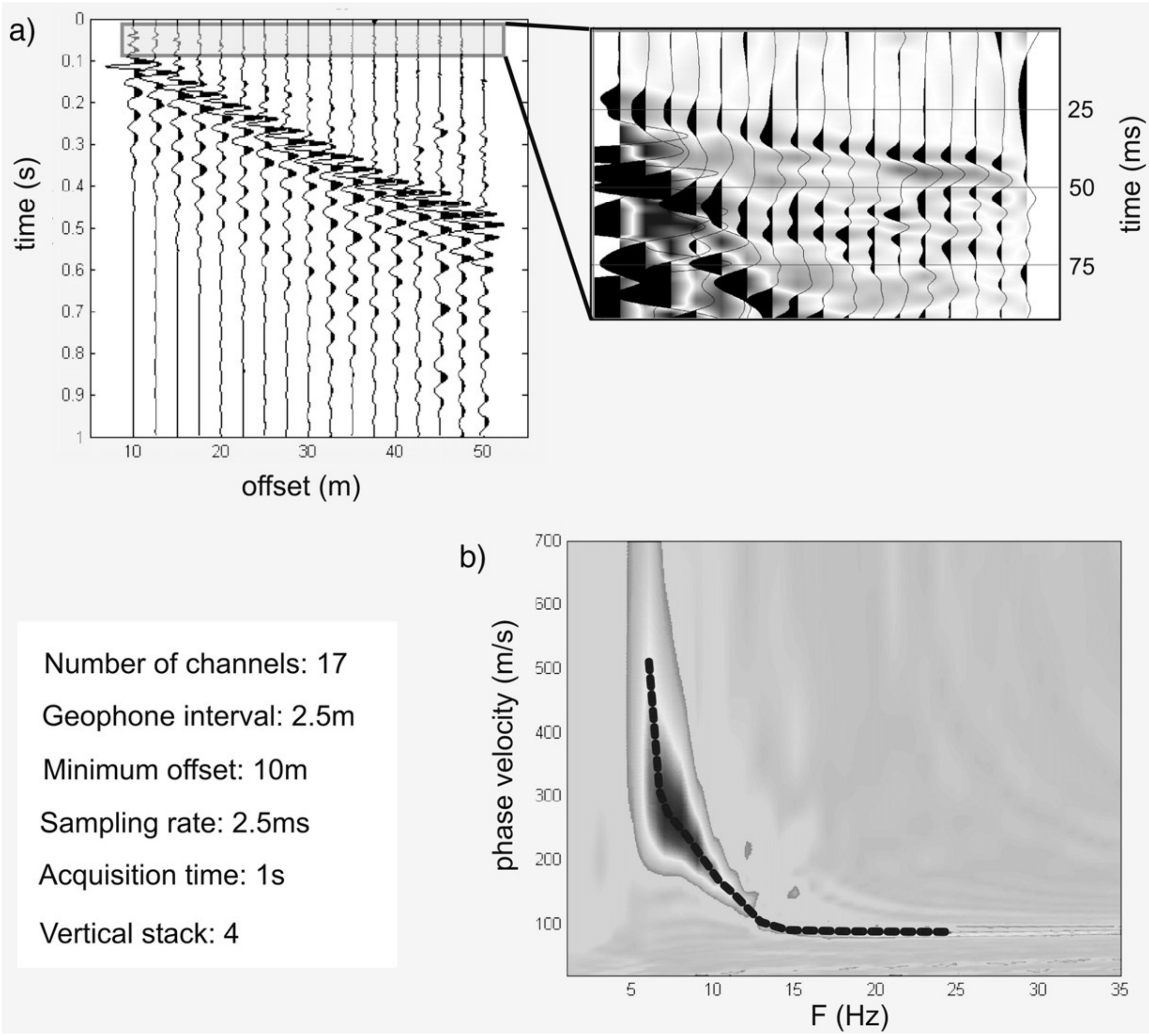

Fig. 7. Field dataset: (a) common-shot gather (with a close-up on the first arrivals) and (b) its velocity spectrum (with highlighted the picked dispersion curve).

From these initial considerations a number of inversions based on a 3-layer model and with various Poisson values were performed.

The asymmetric distribution of the Pareto front models obtained for all the performed inversions (for the sake of brevity we will not present the results of all the performed inversion but a representative example is reported in Fig. 9) gives evidence of a fundamentally-incorrect provisional interpretation.

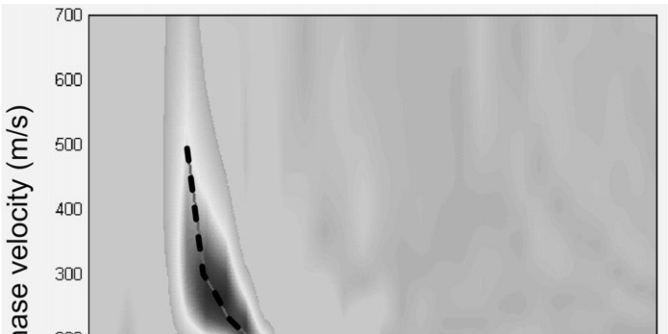

Fig. 8. Observed velocity spectrum and dispersion curve for a 3-layer model (V_S = 87, 335 and 1014 m/s and THK = 3.5 and 4 m).

A further set of possible interpretative hypotheses were then tested in order to identify a good (i.e. symmetrical) distribution of the Pareto front models (evidence of a proper interpretative hypothesis).

We decided to adopt a 4-layer model with the two refractions attributed to the two deepest interfaces.

A major problem was the determination of the Poisson ratios to adopt as the results of several inversions performed with different values proved that the procedure is quite sensitive to such parameter. As also the synthetic tests put in evidence, erroneous Poisson values determine V_P values that cannot produce the correct (observed) travel times. This fact generates an asymmetric distribution of the Pareto front models similar to the ones reported in Figs. 5a and 9a, being the amount of asymmetry somehow proportional to the error.

The results obtained while attributing the Poisson value sequence {0.48, 0.47, 0.46, 0.26} (from top to bottom), with ±4% of allowed tolerance (see Table 6) are reported in Fig. 10. Model distribution, Pareto front symmetry, observed and calculated dispersion curves and refraction travel times (compare Figs. 9 and 10) altogether demonstrate a good and coherent provisional interpretation (retrieved mean model is summarized in Table 6). The limited Pareto front spread is easily explained by a small amount of noise or minor lateral variations (see also Dal Moro and Pipan, 2007).

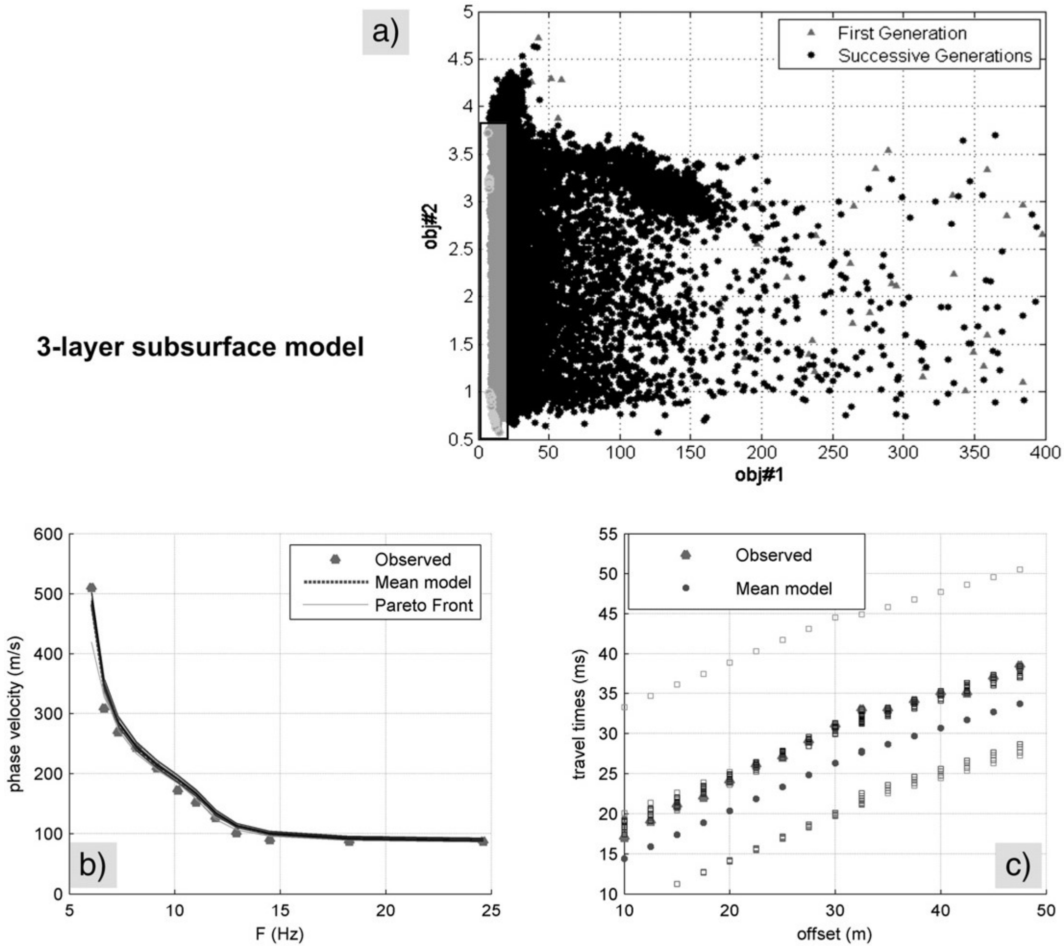

Fig. 9. Bi-objective inversion performed considering a 3-layer Earth model: (a) model distribution in the objective space (Pareto front models highlighted by circles within the rectangle); (b) and (c) observed and calculated dispersion curves and refraction travel times.

From the evaluation of the velocities and Poisson ratio values of the retrieved model (Table 7) we can infer that the first two layers are sands that very likely differ in grain size, pressure and water content (see Prasad, 2002 and Zimmer et al., 2002) while the third one is very likely to be made up of water-sutured gravels. The underlying half-space clearly exhibits characteristics of hard rock.

5. Conclusions

Any sort of data is able to cast light only onto a specific aspect of the investigated problem. The implementation of a joint inversion scheme is meant to proficiently integrate the information that can be extracted from one dataset with those coming from another one. If the two objectives depend upon the same variables we can obtain a better-focused solution, while if the two objectives pertain (even just partially) to different variables thus their joint use can lead to new considerations characterized by a higher so-to-speak added value.

Table 6
Interpretative hypothesis and search space considered for the bi-objective inversion reported in Fig. 10 (the two retraction travel times are attributed to the two deepest interfaces)

		Poisson (±4%)	Search space	
			V_S (m/s)	THK (m)
Layer	1	0.48	80÷120	0.5÷3
	2	0.47	40÷100	1÷3.5
	3	0.46	100÷600	4÷10
	4	0.26	1200÷1700	*half-space*

In this study we analysed *ground roll* and refracted waves, which are the most evident events in common-shot gathers obtained from standard vertical-geophone surveys.

Ground roll allows the determination of the Rayleigh wave dispersion curve while first breaks the compilation of the time-distance curves for direct/refracted waves.

Such information can lead to infer three fundamental parameters: shear-wave velocity, which is the most influential parameter in Rayleigh wave dispersion; compressional wave velocity, which affects the first arrivals of refracted waves; layer thickness, which is a crucial parameter for both events (surface-wave propagation and refracted P-waves).

Two points are nevertheless relevant, one pertaining to the refraction travel times the other one to the dispersion curve.

As well known, in spite of the extensive use of refraction travel times in applied studies aimed at defining subsurface discontinuities, first breaks are often hard to read and some interpretive hypothesis is always necessarily adopted. Results of refraction data interpretation are therefore prone to failures.

On the other hand, dispersion curve inversion suffers from severe non-uniqueness (which actually affects refraction as well), i.e. different models are compatible with a given dispersion curve.

The consequence is that retrieving a model from refraction travel times or dispersion curves alone is often risky and/or can provide wrong or approximate models.

The proposed joint inversion scheme is based on a bi-objective evolutionary algorithm which exploits the Pareto criterion (Dal Moro

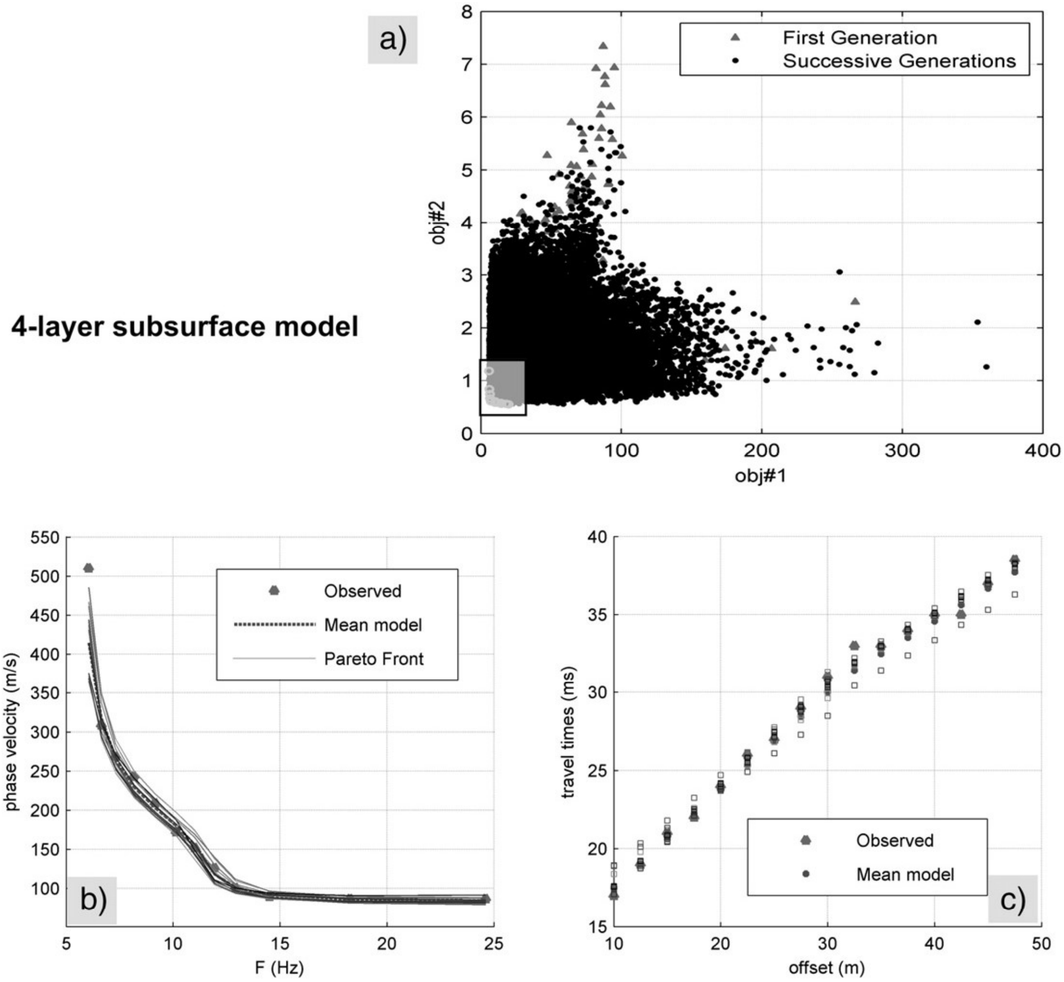

Fig. 10. Results of the bi-objective inversion accomplished while considering the 4-layer interpretative hypothesis summarized in Table 6. (a) model distribution in the objective space (Pareto front models highlighted by circles within the rectangle), (b) and (c) observed and calculated dispersion curves and refraction travel times.

and Pipan, 2007). The methodology allows the determination of the vertical velocity profiles (shear and compressional waves) and Poisson ratio as a by-product.

In the presented procedure, Poisson ratios are fixed by the user (together with a percentage of tolerance) and the results are then eventually able to confirm or discharge the adopted hypotheses. In case Poisson values are excessively far from the true ones, the resulting Pareto front models appears asymmetric (with respect to the rest of the model distribution — see e.g. Figs. 5 and 9) and different values should be adopted and tested.

The problem is particularly tricky because the optimization procedure is quite sensitive and even small errors of the initially-assumed Poisson values (to be successively tuned by the inversion procedure) can determine serious effects in the final results.

As a consequence, especially when dealing with field datasets (necessarily including a variable amount of noise), joint inversion can be hard to parameterize but, on the other hand, final results appear to be quite robust.

Symmetric distribution of the Pareto front models gives evidence of a proper interpretative hypothesis while asymmetry is caused by unbalanced V_P–V_S and/or geometrical relationships due to erroneous interpretation (number of layers, refractor attribution, assumed Poisson values).

Some points regarding the evaluation of the Pareto front models should be underlined. In MOPs (Multi-Objective Problems) the final solution is not a single model but a set of "Pareto Optimal Models" (POMs) which are perfectly equivalent in terms of "goodness" (of course for practical use it is possible to summarize final POMs in a single mean model). Among the POMs it is not possible to determine a model “fitter” than the others. They all together represent the best set of solutions for the given problem (see Fonseca and Fleming, 1993; Van Veldhuizen and Lamont, 1998a,b, 2000; Coello Coello 2002, 2003).

The good misfit of the dispersion curves both in case of proper or wrong interpretation (compare case #1 and case #2) is a clear evidence of the well-known problem of non-uniqueness in dispersion curve inversion (different models can be equivalent in terms of surface wave dispersion curves). This is why special attention should be paid when dealing with studies carried out using surface wave analysis only.

A crucial point of the present work is that Pareto front symmetry gives the opportunity to estimate whether the provisional interpretative hypothesis [i.e. number of layers, Poisson values, allowed (or not) presence of a low-velocity layer, refraction attribution to a certain horizon] is appropriate or not.

Table 7
Mean model obtained from the inversion presented in Fig. 10 and Table 6

		V_P (m/s)	V_S (m/s)	THK (m)	Poisson
Layer	1	1124	90	1.7	0.497
	2	376	82	1.8	0.475
	3	1597	453	6.4	0.456
	4	2385	1357	*half-space*	0.261

The determination of the Pareto front symmetry (which is evaluated with respect to the totality of the models in the objective space and consequently does not depend on the adopted units of measurements) is then a kind of coherency test: once we eventually determine the final set of POMs we have the chance to evaluate their consistency with respect to the observed data by evaluating the Pareto front symmetry.

A synthetic case including a hidden layer was initially considered in order to assess the performances of the algorithm in challenging conditions, i.e. where one of the two methods (refraction analysis) is bound to fail. A field dataset obtained with vertical geophones and vertically-incident seismic source was then analysed.

The adopted methodology has proved to furnish good results able to depict the subsurface conditions of the investigated area in terms of V_S and V_P vertical profiling.

It is worth noticing that V_P and V_S need careful evaluation with respect to water content. The relationship between water saturation and shear-wave velocity is quite complex but as a general rule an increase in water content should reflect in a decrease in V_S (e.g. Dvorkin, 2008), while for near-surface unconsolidated sediments compressional-wave velocity typically increases.

The proposed inversion scheme is able to cope with this aspect (variation in the V_P/V_S ratio due to variation in water content). Changes due to variations in water saturation in a homogeneous layer are in fact modelled by using two layers with different Poisson moduli.

The application of the presented inversion scheme in a real case has shown that the proposed approach can be actually successfully applied in challenging subsurface conditions.

For the analysed field dataset, if dispersion curve and refraction travel times were analysed separately, an incoherent 3-layer model would have been determined. A more complex 4-layer hypothesis was proficiently handled in the frame of the proposed MOEA inversion scheme and led to the determination of a subsurface model where a low-velocity layer below the uppermost one is present.

Acknowledgements

This research was supported by research grants COFIN 2004 and COFIN 2006 and a grant for the Algeria-Italy bilateral project "Development of integrated geological-geophysical methodologies for the evaluation of seismo-tectonic risk in the *Petite Kabylie* region" (Algeria).

The author was also awarded of a fellowship by the *Progetto D4* (European Social Fund, Italian Ministry of Welfare and Regione Friuli Venezia Giulia).

The author wishes to express his sincere gratefulness to Julian Ivanov for his comments and suggestions while reviewing the paper.

References

Coello Coello, C.A., 2002. Evolutionary Multiobjective Optimization: Past, Present and Future. Open file, http://www.cs.cinvestav.mx/~EVOCINV/download/tutorial-moea.pdf.

Coello Coello, C.A., 2003. Guest editorial: special issue on evolutionary multiobjective optimization. IEEE Trans. Evol. Comp. 7, 97–99.

Dal Moro, G., Pipan, M., 2007. Joint Inversion of Surface Wave Dispersion Curves and Reflection Travel Times via Multi-Objective Evolutionary Algorithms. J. Appl. Geophys. 61, 56–81.

Dal Moro, G., Forte, E., Pipan, M., Sugan, M., 2006. Velocity Spectra and Seismic Signal Identification for Surface Wave Analysis. Near-Surface Geophys. 4, 243–251.

Dal Moro, G., Pipan, M., Gabrielli, P., 2007. Rayleigh Wave Dispersion Curve Inversion via Genetic Algorithms and Marginal Posterior Probability Density Estimation. J. Appl. Geophys. 61, 39–55.

Dvorkin, J.P., 2008. Yet another V_S equation. Geophysics 73, E35–E39.

Evison, F.F., Orr, R.H., Ingham, C.E., 1959. Thickness of the earth's crust in Antarctica. Nature 183, 306–308.

Fonseca, C.M., Fleming, P.J., 1993. Genetic Algorithms for Multiobjective Optimization: Formulation, Discussion and Generalization. Proceeding of the fifth International Conference on Genetic Algorithms. Morgan Kauffman, San Mateo, CA (USA), pp. 416–423.

Gardner, G.H.F., Gardner, L.W., Gregory, A.R., 1974. Formation velocity and density —The diagnostic basic for stratigraphic trap. Geophysics 39, 770–780.

Gerstoft, P., Mecklenbrauker, C.F., 1998. Ocean acoustic inversion with estimation of a posteriori probability distributions. J. Acoust. Soc. Am. 104, 808–819.

Glangeaud, F., Mari, J., Lacoume, J.-L., Mars, J., Nardin, M., 1999. Dispersive Seismic Waves in Geophysics. Eur. J. Env. Engineer. Geophys. 3, 265–306.

Goldberg, D.E., 1989. Genetic Algorithms in Search, Optimization, and Machine Learning. Addison-Wesley Publishing Company, Inc.. 412 pp.

Ivanov, J., Miller, R.D., Xia, J., Steeples, D., Park, C.B., 2006. Joint Analysis of Refractions with Surface Waves: An Inverse Refraction-Traveltime Solution. Geophysics 71, R131–R138.

Ivanov, J., Miller, R.D., Xia, J., Steeples, D., Park, C.B., 2005a. The inverse problem of refraction traveltimes, part I: Types of geophysical nonuniqueness through minimization. Pure Appl. Geophys. 162, 447–459.

Ivanov, J., Miller, R.D., Xia, J., Steeples, D., 2005b. The inverse problem of refraction traveltimes, part II: Quantifying refraction nonuniqueness using a three-layer model. Pure Appl. Geophys. 162, 461–477.

Louie, J.N., 2001. Faster, Better: Shear-Wave Velocity to 100 Meters Depth from Refraction Microtremor Arrays. BSSA 91, 347–364.

Luke, B., Calderón-Macías, C., Stone, R.C., Huynh, M., 2003. Nonuniqueness in inversion of seismic surface-wave data. Proceedings on the Symposium on the application of geophysics to engineering and environmental problems, Environmental and Engineering Geophysical Society,. CD-ROMSUR05.

Man, K.F., Tang, K.S., Kwong, S., 2001. Genetic Algorithms. Springer. 344 pp.

Park, C.B., Miller, R.D., Xia, J., 1999. Multichannel analysis of surface waves. Geophysics 64, 800–808.

Prasad, M., 2002. Acoustic measurements in unconsolidated sands at low effective pressure and overpressure detection. Geophysics 67, 405–412.

Robertsson, J.O.A., Pugin, A., Holliger, K., Green, A.G., 1995. Effects of near-surface waveguides on shallow seismic data. 65th SEG, Meeting, Houston, USA, Expanded Abstracts, pp. 1329–1332.

Roth, M., Holliger, K., 1999. Inversion of source-generated noise in high-resolution seismic data. Lead. Edge 18, 1402–1406.

Soske, J.L., 1959. The blind zone problem in engineering geophysics. Geophysics 24, 359–365.

Stokoe II, K.H., Nazarian, S., Rix, G.J., Sanchez-Salinero, I., Sheu, J., Mok, Y., 1988. In situ seismic testing of hard-to-sample soils by surface wave method. Earthq. Eng. and Soil dyn. II — Recent adv. in ground-motion eval. ASCE, Park City, pp. 264–277.

Van Veldhuizen, D.A., Lamont, G.B., 2000. Multiobjective Evolutionary Algorithms: Analyzing the State-of-the-Art. Evol. Comput. 8, 125–147.

Van Veldhuizen, D.A., Lamont, G.B., 1998a. Multiobjective Evolutionary Algorithms: A History and Analysis. Air Force Institute of Technology, Technical Report TR-98-03. 88 pp.

Van Veldhuizen, D.A., Lamont, G.B., 1998b. Evolutionary Computation and Convergence to a Pareto Front. In: Koza, John R. (Ed.), Late Breaking Papers at the Genetic Programming 1998 Conference. Stanford University, pp. 221–228.

Soft Computing for Reservoir Characterization and Modeling. In: Wong, P., Aminzadeh, F., Nikravesh, M. (Eds.), Series Studies in Fuzziness and Soft Computing, vol 80. Springer, Physica-Verlag. 586 pp.

Xia, J., Miller, R.D., Park, C.B., 1999. Estimation of near-surface shear-wave velocity by inversion of Rayleigh waves. Geophysics 64, 691–700.

Zhang, S.X., Chan, L.S., 2003. Possibile effects of misidentified mode number on Rayleigh wave inversion. J. Appl. Geophys. 53, 17–29.

Zimmer, M., Prasad, M., Mavko, G., 2002. Pressure and porosity influences on V_P–V_S ratio in unconsolidated sands. Lead. Edge 21, 178–183.